Stem Cell Reports Article



-OPEN ACCESS

MAGIK: A rapid and efficient method to create lineage-specific reporters in human pluripotent stem cells

Tahir Haideri, ¹ Jirong Lin, ¹ Xiaoping Bao, ^{4,*} and Xiaojun Lance Lian ^{1,2,3,5,*}

- ¹Department of Biomedical Engineering, Pennsylvania State University, University Park, PA 16802, USA
- ²Huck Institutes of the Life Sciences, Pennsylvania State University, University Park, PA 16802, USA
- ³Department of Biology, Pennsylvania State University, University Park, PA 16802, USA
- ⁴Davidson School of Chemical Engineering, Purdue University, West Lafayette, IN 47907, USA
- Lead contact

*Correspondence: bao61@purdue.edu (X.B.), lian@psu.edu (X.L.L.)

https://doi.org/10.1016/j.stemcr.2024.03.005

SUMMARY

Precise insertion of fluorescent proteins into lineage-specific genes in human pluripotent stem cells (hPSCs) presents challenges due to low knockin efficiency and difficulties in isolating targeted cells. To overcome these hurdles, we present the modified mRNA (ModRNA)-based Activation for Gene Insertion and Knockin (MAGIK) method. MAGIK operates in two steps: first, it uses a Cas9-2A-p53DD modRNA with a mini-donor plasmid (without a drug selection cassette) to significantly enhance efficiency. Second, a deactivated Cas9 activator modRNA and a 'dead' guide RNA are used to temporarily activate the targeted gene, allowing for live cell sorting of targeted cells. Consequently, MAGIK eliminates the need for drug selection cassettes or labor-intensive single-cell colony screening, expediting precise gene editing. We showed MAGIK can be utilized to insert fluorescent proteins into various genes, including *SOX17*, *NKX6.1*, *NKX2.5*, and *PDX1*, across multiple hPSC lines. This underscores its robust performance and offers a promising solution for achieving knockin in hPSCs within a significantly shortened time frame.

INTRODUCTION

CRISPR-mediated gene knockin methodologies have emerged as powerful tools for gene editing (Banan, 2020; Lau et al., 2020), marking significant strides in improving efficiency, specificity, and the scope of targeting. CRISPR-Cas9 can introduce precise double-stranded breaks (DSBs) in targeted DNA sites (Cong et al., 2013; Jinek et al., 2012; Mali et al., 2013), thereby enabling the insertion of specific genetic variant sequences provided by the donor DNA templates. Of note, homology-directed repair (HDR) is a major mechanism that aids this process (Capecchi, 1989). HDR permits the precise integration of exogenous DNA sequence at a specific site in the genome where a DSB has occurred (Azhagiri et al., 2021; Hsu et al., 2014). The HDR process relies heavily on donor DNA templates, which come in three primary forms: double-stranded DNA (dsDNA) (Merkle et al., 2015; Yu et al., 2020; Zhang et al., 2017), single-stranded DNA (ssDNA) (Kagita et al., 2021; Okamoto et al., 2019; Yoshimi et al., 2016), and adeno-associated virus (AAV) (Bak and Porteus, 2017; Gaj et al., 2017). While ssDNA and AAV may enhance knockin efficiency in comparison with dsDNA, the latter is simpler to manufacture and produce.

A recent advancement in CRISPR-mediated gene knockin technology entails the integration of fluorescent proteins into lineage-specific marker genes within human pluripotent stem cells (hPSCs) (Cruz-Santos et al., 2022; Martyn et al., 2018; Sluch et al., 2015; Wu et al., 2018). The creation of fluorescent reporter lines has revolutionized the isola-

tion process of desired differentiated cells and offers an invaluable tool for refining conditions to enhance stem cell differentiation (Bao et al., 2019; Den Hartogh and Passier, 2016). Fluorescent reporters offer the ability to illuminate specific cell populations, thereby enabling real-time tracking of cell type specification throughout the differentiation. For instance, the knockin of EGFP into the endogenous NKX2.5 locus (Elliott et al., 2011) in hPSCs generates lines that express EGFP concurrent with the emergence of cardiac progenitors during cardiac differentiation of hPSCs. The advantage of real-time monitoring and tracking of particular cell populations lies in the opportunity it provides for uncovering the molecular mechanisms underlying the differentiation of hPSCs into defined cell types.

An alternative method for generating reporter cell lines for lineage specific marker genes involves the non-specific insertion of fluorescent transgenes under control of gene-specific promoters via retro/lentiviral-mediated integration (Ovchinnikov et al., 2014; Sun et al., 2016). However, as opposed to targeted insertion of the fluorescent reporter at the endogenous locus, this method is limited to known proximal regulatory regions and may not fully capture the diverse gene regulatory elements that play a role in endogenous gene expression, including but not limited to distal enhancers and chromatin state, producing a less faithful reporter cell population (Liu et al., 2018). Additionally, the silencing of transgenes delivered via retro/lentiviral methods has been well documented in hPSCs, making them less than ideal vectors for the generation of reporter lines (Cabrera et al., 2022; Herbst et al., 2012; Xia et al., 2007).





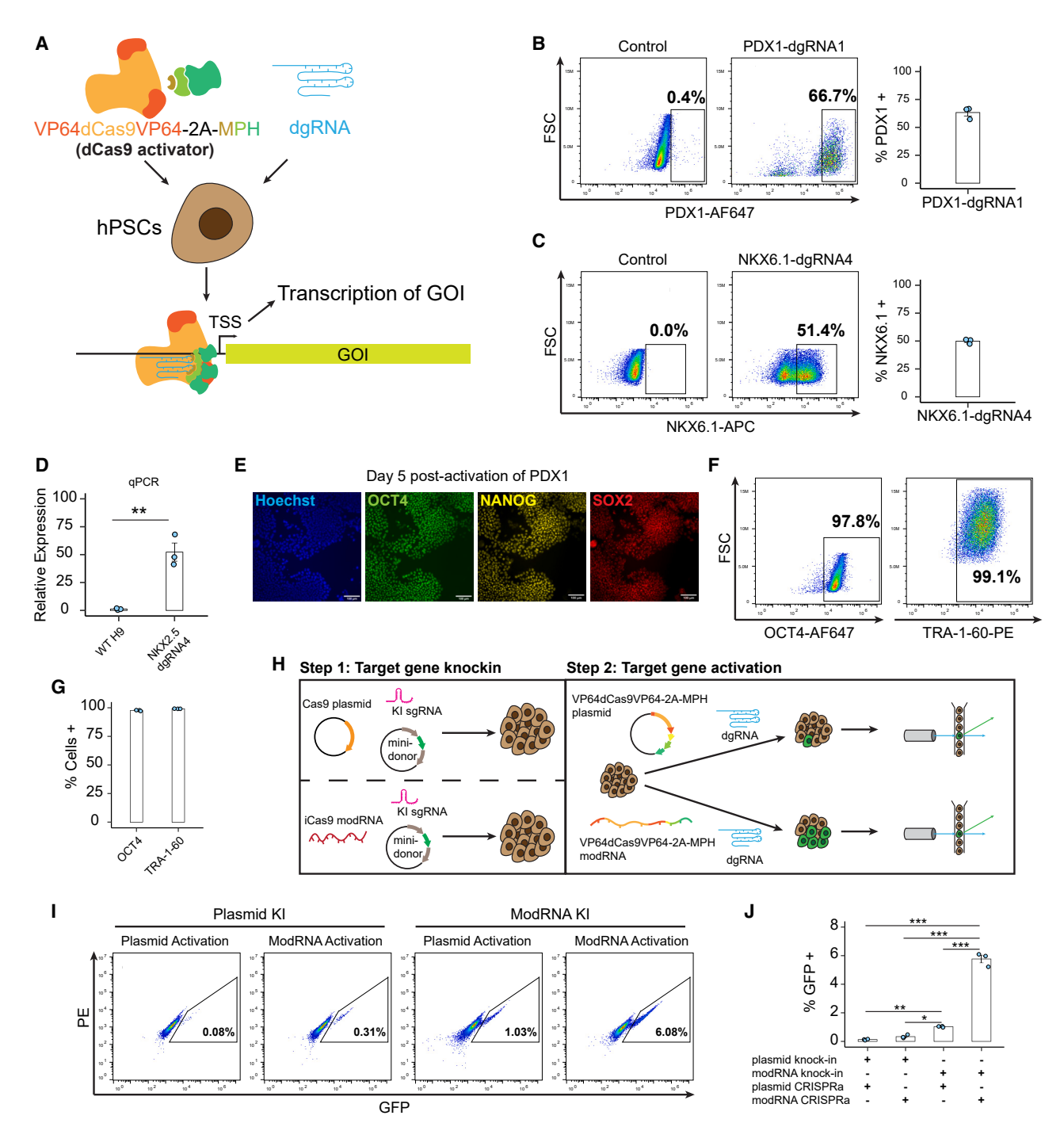


Figure 1. ModRNA delivery increased gene knockin and target gene activation

(A) Schematic diagram for dCas9 activator mediated activation of silenced genes.

(B and C) WT H9 cells were transfected with dCas9 activator modRNA and either PDX1 dqRNA (B) or NKX6.1 dqRNA (C). Cells were collected 48 h after transfection and analyzed for PDX1 (B) or NKX6.1 (C) expression by flow cytometry. The bar chart shows the mean % positive cells and error bars representing SEM across three independent experiments.

(D) WT H9 cells were transfected with dCas9 activator modRNA and NKX2.5 dqRNA. Cells were collected for qPCR analysis of NKX2.5, 48 h after transfection. Relative expression of NKX2.5 is shown in transfected cells vs. untransfected cells.

(E-G) WT H9 cells were transfected with dCas9 activator modRNA and PDX1 dgRNA. Five days later, cells were immunostained for OCT4, NANOG, SOX2, and TRA-1-60 and analyzed by either immunofluorescent imaging (E) or flow cytometry (F and G). Scale bar, 100 μm.

(legend continued on next page)



Due to the inherently low efficiency of traditional HDRmediated knockin, a drug selection cassette (e.g., PGK-Puro^R) was commonly included in the donor vector. This addition allows for the enrichment of targeted clones. Despite this improvement, the efficiency remains relatively low, necessitating the screening of hundreds of drug-resistant clones. For example, in the case of OCT4-EGFP knockin, researchers selected 288 puromycin-resistant clones and subsequently performed PCR and Southern blot analysis to identify only eight correctly targeted clones (2.8% efficiency) (Zhu et al., 2015). A major challenge posed by this drug selection approach is that the drug selection cassette interferes with the expression of the integrated fluorescent protein (Zhu et al., 2015). Consequently, an additional step is necessary to remove the drug selection cassette after successful knockin, which can significantly slow down the generation of hPSC reporter lines.

To address this, the use of a drug selection cassette-free donor vector has been proposed, aiming to expedite the process. However, this selection-free approach may result in even lower efficiency. Furthermore, for lineage-specific genes, the lack of fluorescence in successfully targeted cells precludes the use of live cell fluorescence-activated cell sorting (FACS) technology for isolating knockin cells. As a workaround, a traditional post-knockin process is adopted: cells are replated at a single cell density, left for approximately 10 days, and then single cell-derived clones are selected. A subsequent genomic PCR analysis verifies the successful knockins. As a result, inserting fluorescent proteins into lineage-specific marker genes in hPSCs remains a significant challenge.

To address these challenges, we have developed a novel strategy: modified mRNA (modRNA)-based Activation for Gene Insertion and Knockin (MAGIK). MAGIK is designed to both enhance knockin efficiency and simplify the process of isolating successfully targeted cells. Our MAGIK method starts with the use of a Cas9-2A-p53DD modRNA, an alternative to the Cas9 plasmid, to significantly enhance knockin efficiency. The subsequent step uses a deactivated Cas9 (dCas9) activator modRNA to temporarily activate the expression of lineage-specific gene and its associated fluorescent protein. CRISPR activation (CRISPRa) was recently used to enhance transgene enrichment in a study conducted by Mikkelsen et al. (2023). In their research, they incorporated CRISPRa target (the miniCMV reporter gene), and their gene of interest (GOI) into the same HDR template

(Mikkelsen et al., 2023). Consequently, CRISPRa of the miniCMV-reporter gene cassette indicated successful knockin of the GOI (Mikkelsen et al., 2023). This approach differs significantly from our MAGIK method. In MAGIK, we directly target the reporter gene into a lineage-specific gene and identify knockin cells by activating this lineagespecific gene using CRISPRa. This maneuver simplifies cell isolation through FACS, negating the need for selection of single cell-derived clones. By circumventing the necessity for the selection and genomic PCR of single cellderived clones, our approach provides a markedly efficient and expedited alternative to conventional methods.

RESULTS

ModSAM system robustly activates silenced gene expression in hPSCs

CRISPRa systems (Chavez et al., 2016; Kiani et al., 2015; Konermann et al., 2015) are extensively used to initiate the transcription of otherwise silenced genes in a manner specific to gRNAs. In earlier work (Haideri et al., 2022), we showed how the gene editing efficiency in hPSCs could be increased through a modRNA-based delivery of Cas9, which resulted in up to a 3-fold increase over an equivalent plasmid-based strategy. With this success, we chose to adapt our modRNA-based approach to the CRISPRa system in hPSCs. We decided to develop modRNA-based synergistic activation mediator (modSAM) system (Figure 1A). Our modSAM system is composed of two key components. The first is the dCas9 activator modRNA (VP64dCas9VP64-2A-MPH), which utilizes two VP64 transcriptional activators, each attached to the N and C terminus of the dCas9. It also includes the expression of the MS2-p65-HSF1 (MPH). The second component is an engineered 'dead' guide RNA (dgRNA) (Liao et al., 2017). This dgRNA is unique as it contains two MS2 aptamers and has a spacer length of 14 base pairs (bp). A notable advantage of using this dgRNA is its ability to pair with either a dCas9 or a catalytically active Cas9 without causing DSBs. By applying our mod-SAM system, we managed to achieve robust activation of lineage-specific genes, NKX6.1, PDX1, and NKX2.5 in hPSCs (Figures 1B-1D). After modSAM transfection using PDX1-dgRNA1, $63.3\% \pm 3.1\%$ PDX1⁺ cells were generated and measured by flow cytometry at 48 h after transfection (Figure 1B). For NKX2.5 activation, we conducted qPCR

Representative plots showing day 5 expression of OCT4 and TRA-1-60. (G) Quantification of (F) with error bars representing SEM across three independent replicates.

⁽H) Diagram of our two-step approach for deriving reporter hPSCs using either plasmid or modRNA transfection.

⁽I and J) NKX2.5-nEGFP reporter cells were generated from WT H9 cells as shown in (H). Cells were analyzed for EGFP expression by flow cytometry, 48 h after activating NKX2.5. (I) Representative plots showing EGFP expression across each of the four combinations.

⁽J) Quantification of (I) with error bars representing SEM across 3 independent experiments. *p < 0.05, **p < 0.01, ***p < 0.001.



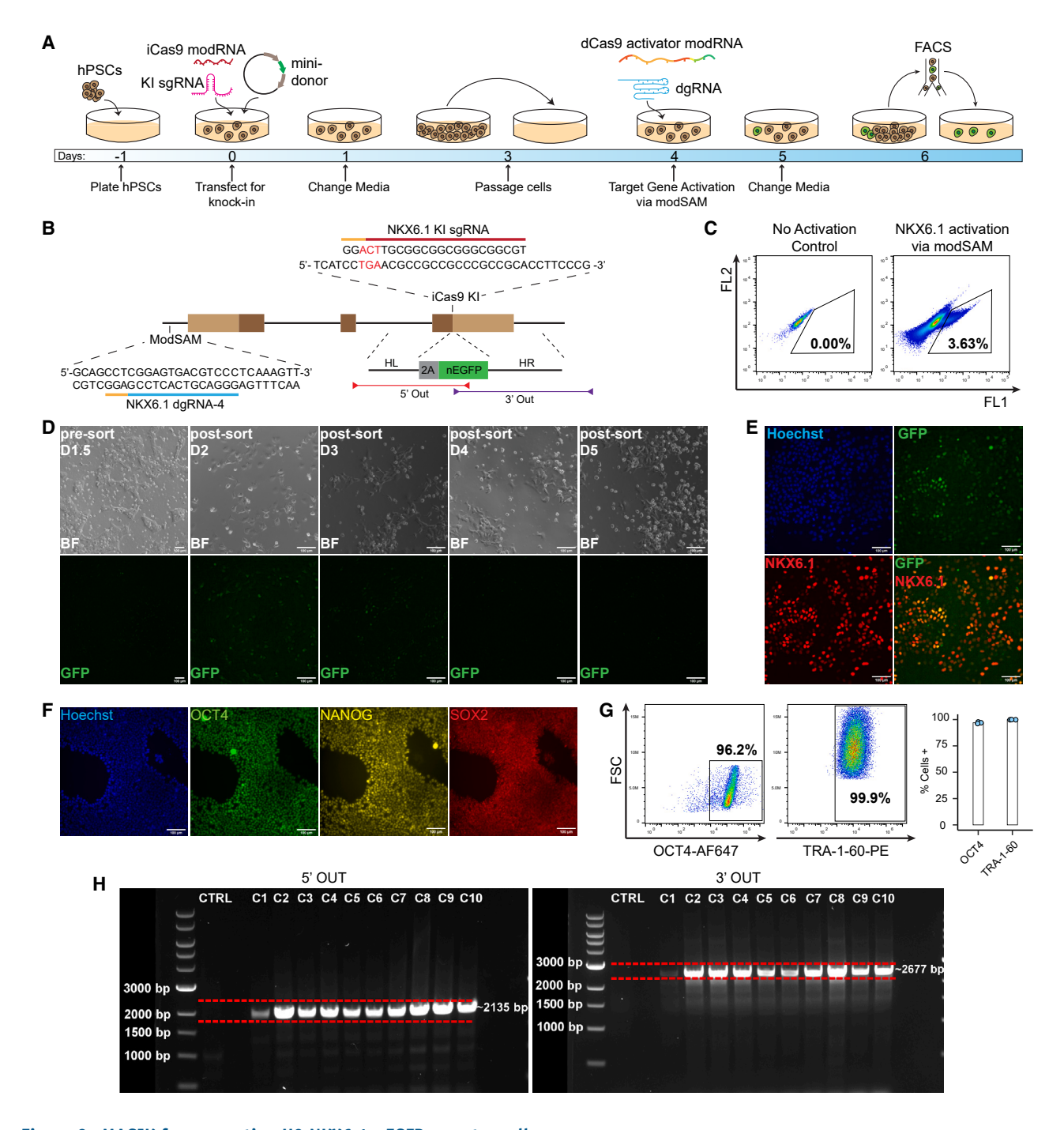


Figure 2. MAGIK for generating H9 NKX6.1-nEGFP reporter cells

- (A) Schematic diagram showing timeline for MAGIK approach.
- (B) Diagram showing knockin and activation strategy.
- (C) WT H9 cells were transfected with iCas9 modRNA, NKX6.1 KI sgRNA, and NKX6.1-nEGFP mini-donor plasmid. The mixed knockin cells were transfected with dCas9 activator modRNA and NKX6.1 dgRNA. EGFP⁺ cells were sorted via FACS 48 h after transfection and replated into 1 well of a 48-well plate. Representative plot showing percentage of EGFP-positive cells.
- (D) Representative brightfield and fluorescent images of knockin reporter cells before and after sorting until day 5 post-transfection. Scale bar, 100 μ M.
- (E) Post-sort H9 NKX6.1-nEGFP reporter cells were transfected with dCas9 activator modRNA and NKX6.1 dgRNA. On day 2 after transfection, cells were fixed and stained for NKX6.1. Scale bar, 100 μ M.

(legend continued on next page)



analysis after modSAM transfection, demonstrating up to a 68-fold increase in NKX2.5 expression compared with the untransfected hPSCs (Figure 1D).

While activation with our modSAM initially induced morphological changes in cultured hPSCs, we observed that cells reverted to the typical hPSC morphology 4-5 days later. Consequently, we decided to evaluate whether hPSCs maintain pluripotency 5 days after transfection by analyzing the expression of pluripotency markers. Nearly 100% of day 5 cells were positive for OCT4, NANOG, and SOX2 based on immunostaining assays (Figures 1E and S1A). This was confirmed by flow cytometry analysis of day 5 cells, which showed high levels of OCT4 and TRA-1-60 expression similar to wild-type (WT) hPSCs (Figures 1F, 1G, and S1B-S1E). Considering the transient nature of the activation and the absence of irreversible differentiation in the modSAM transfected cells, we hypothesized that our modSAM system might serve as a selection tool for purifying targeted cells after Cas9-mediated knockin of fluorescent proteins to lineage-specific genes. At present, the selection for successful knockin of lineage-specific genes necessitates a laborious process involving the selection and validation of singlecell clones through genomic PCR and sequencing.

To test our proposed strategy and show the efficacy of our modRNA-based approach against traditional plasmid-based methods, we designed an experiment to create EGFP with nuclear localization signal sequence (NKX2.5-nEGFP) reporter cells using parallel methods of plasmid-based or modRNA-based delivery of Cas9 and dCas9 activator (Figure 1H).

Our MAGIK strategy uses a two-step approach: first, we use a Cas9-2A-p53DD modRNA (iCas9 modRNA), a sgRNA targeting the stop codon region (KI sgRNA), and a minidonor plasmid (no drug selection cassette) to insert the fluorescent protein. The iCas9 modRNA was used because it can generate higher gene editing efficiency as compared with Cas9 modRNA (Figure S1F). Subsequently, we transiently activate the target gene using modSAM to enable sorting of the positive cells.

For our initial screen, we performed each step using either plasmid-based or modRNA-based delivery, yielding a total of four possible combinations. We analyzed the efficiency of each combination via flow cytometry of activated cells. Consistent with our initial hypothesis, our modRNA-based approach for both steps significantly outperformed all other combinations, showing a nearly 45-fold improvement over

an entirely plasmid-based approach (5.77% \pm 0.27% vs. $0.13\% \pm 0.03\%$) (Figures 1I and 1J). We validated our results in a second gene via generation of PDX1-EGFP reporter cells. We observed a 15-fold improvement with our modRNAbased strategy over the traditional plasmid-based delivery of CRISPR components (Figures \$1G and \$1H).

Generation of the NKX6.1-nEGFP reporter line via **MAGIK**

Considering the effectiveness of our approach in achieving significantly higher proportions of targeted cells, we chose to utilize our MAGIK method to create an NKX6.1nEGFP H9 reporter line (Figure 2A). NKX6.1 is an important marker for pancreatic progenitors and beta cells (Lee et al., 2019; Pagliuca et al., 2014). We cloned an NKX6.1-nEGFP mini-donor plasmid (no drug-selection cassette), based on the traditional NKX6.1 donor plasmid previously reported (Liu et al., 2021). Additionally, we synthesized a KI sgRNA targeting the stop codon region of NKX6.1 based on a published sequence (Liu et al., 2021) (Figure 2B).

H9 cells were initially transfected with iCas9 modRNA, NKX6.1 KI sgRNA, and NKX6.1-nEGFP mini-donor plasmid. After a cultivation period, cells were passaged and transfected with our modSAM system (dCas9 activator modRNA + NKX6.1-dgRNA4). Two days after transfection, EGFP+ cells were sorted and replated. The purity of EGFP⁺ cells was 3.63%, compared with 0% in the untransfected population (Figure 2C). We confirmed EGFP expression via fluorescent microscopy on the day of sorting (Figure 2D). Subsequently, all cells were EGFP⁻ on day 5 after transfection (Figure 2D).

To assess whether the sorted cells were indeed NKX6.1nEGFP knockin cells, we transfected the sorted cells via modSAM and immunostained the cells using a NKX6.1 antibody. Our data showed co-localization of EGFP with anti-NKX6.1 antibody signal (Figure 2E). To study whether the sorted cells retained pluripotency, we assessed the cells via immunostaining of pluripotency makers. Our data showed the sorted cells exhibited nearly 100% expression of OCT4, NANOG, and SOX2 (Figure 2F), with flow cytometry revealing similar expression levels of OCT4 and TRA-1-60 to WT H9 cells (Figures 2G, and S1B), qPCR analysis of FACS-isolated H9 NKX6.1-nEGFP showed robust expression of pluripotency markers OCT4, SOX2, and NANOG, while human dermal fibroblasts showed minimal expression (Figure S2A).

(F and G) Post-sort NKX6.1-nEGFP reporter cells were stained for OCT4, NANOG, SOX2 and TRA-1-60 and analyzed by either immunofluorescent imaging (F) or flow cytometry (G). Scale bar, 100 µm. Error bars represent SEM across three independent experiments. (H) PCR genotyping of 10 single-cell-derived clones from post-sort NKX6.1-nEGFP reporter cells. The expected band from each set of primers is highlighted by a pair of red dashed lines (5' OUT, 2,135 bp; 3' OUT, 2,677 bp).



From the sorted cell population, we derived single cell clones and extracted genomic DNA (gDNA). PCR on the gDNA with our 5' Out and 3' Out primers (Figure 2B) confirmed successful integration of EGFP at the expected site in all clonal populations (Figure 2H).

Generation of the SOX17-nEGFP reporter line via MAGIK

SOX17 gene encodes a member of the SOX (SRY-related HMG-box) family of transcription factors. It plays a crucial role in embryo development and serves as a marker for definitive endoderm (DE) (D'Amour et al., 2005; Jiang et al., 2021). Additionally, SOX17 specifies human primordial germ cell (Irie et al., 2015) and blood cell fate (Jung et al., 2021). To generate a SOX17-nEGFP H9 reporter line using our MAGIK method, we cloned a SOX17-nEGFP mini-donor plasmid with the appropriate left and right homology arms (Figure 3A) and synthesized a SOX17 KI sgRNA based on a published sequence (Martyn et al., 2018). The knockin and sorting of EGFP+ cells were performed after modSAM transfection (Figure 2A). During sorting, the purity of EGFP⁺ cells was 0.51% (Figure 3B). After sorting, EGFP+ cells were seeded into one well of the 48-well plate, and EGFP expression was monitored daily until no longer detectable (Figure 3C). Similar to the sorted NKX6.1-nEGFP reporter, all sorted SOX17-nEGFP cells exhibited EGFP expression under fluorescent microscopy (Figure 3C) immediately after sorting. In addition, the sorted cells lost EGFP expression starting from day 4 after sorting (Figure 3C).

To validate whether the sorted cells were indeed SOX17 knockin cells, we transfected the sorted cells via modSAM using a validated SOX17 dgRNA. Our data showed co-localization of EGFP with anti-SOX17 antibody signal (Figure 3D). To assess whether the sorted cells retained an undifferentiated state, we characterized the cells via immunostaining of pluripotency makers. Our data showed the sorted cells exhibited nearly 100% expression of OCT4, NANOG, and SOX2 (Figure 3E), with flow cytometry revealing nearly 100% expression of OCT4 and TRA-1-60 (Figure 3F). We then differentiated the sorted cells into DE cells using our small molecule DE protocol (Jiang et al., 2021). On day 4 of differentiation, the differentiated cells were fixed and immunostained with a SOX17 antibody. Our data revealed that the EGFP expression co-localized with the anti-SOX17 immunofluorescence signal (Figure 3G). To provide further validation of our sorted SOX17-nEGFP H9 reporter line, we performed PCR genotyping of gDNA extracted from 11 single-cell derived clones using our 5' Out and 3' Out primers. Running the PCR product on DNA gels revealed successful integration of the reporter construct in all clonal populations (Figure 3H). Additionally, PCR amplification of gDNA using our Inner primers revealed that all single-cell-derived clones were heterozygous for the fluorescent reporter (Figure 3I).

MAGIK for generation of the NKX2.5-nEGFP reporter

NKX2.5 is a transcription factor that plays a critical role in the specification of cardiac fate, and defects in this gene are associated with congenital heart diseases (Reamon-Buettner and Borlak, 2010). For development of an NKX2.5nEGFP H9 reporter, we synthesized a mini-donor plasmid (Figure 4A). Additionally, we designed and synthesized a NKX2.5 KI sgRNA. H9 cells were transfected with iCas9 modRNA, NKX2.5 KI sgRNA, and NKX2.5-nEGFP minidonor plasmid, followed by modSAM transfection. Two days after modSAM transfection, EGFP+ cells (5.9%) were sorted and seeded onto one well of the 48-well plate (Figure 4B). EGFP expression was monitored via fluorescent microscopy until EGFP expression had completely ablated (Figure 4C). Then we validated our sorted EGFP+ cells via modSAM transfection and immunostaining for NKX2.5 expression. Fluorescent microscopy of immunostained cells showed co-localization of EGFP signal with anti-NKX2.5 antibody signal (Figure 4D). Additionally, sorted reporter cells showed nearly 100% expression of pluripotency markers OCT4, NANOG, and SOX2 as determined by immunostaining (Figure 4E). Flow cytometry of reporter cells stained for OCT4 and TRA-1-60 showed expression equivalent to WT H9 cells (Figures 4F and S1B). NKX2.5nEGFP reporter cells were differentiated into cardiomyocytes using our GiWi protocol (Lian et al., 2012; 2013). Cells assayed on day 10 of differentiation were 74.0% \pm 0.6% EGFP+ according to flow cytometry (Figure 4G). Immunostaining of day 10 cells with anti-NKX2.5 antibody revealed that EGFP signal co-localized with the anti-NKX2.5 antibody (Figure 4H). We derived 12 single-cell clonal lines from the sorted H9 NKX2.5-nEGFP reporter and extracted gDNA for PCR genotyping. Based on the results from our 5' Out and 3' Out primers, we validated successful integration of the reporter construct across all single-cell clonal populations tested (Figures 4I and 4J). Additionally, using our Inner primers we determined that 2 of the 12 clonal populations had bi-allelic integration of the fluorescent reporter (Figure 4K).

MAGIK for generation of the PDX1-EGFP reporter line in multiple hPSC lines

Having demonstrated the effectiveness of MAGIK in creating fluorescent reporter lines spanning various genes within H9 cells, we sought to authenticate our methodology across a spectrum of hPSC lines. To accomplish this objective, we decided to produce PDX1-EGFP reporters utilizing multiple hPSC lines, including H9, H1, IMR90, and 6-9-9.



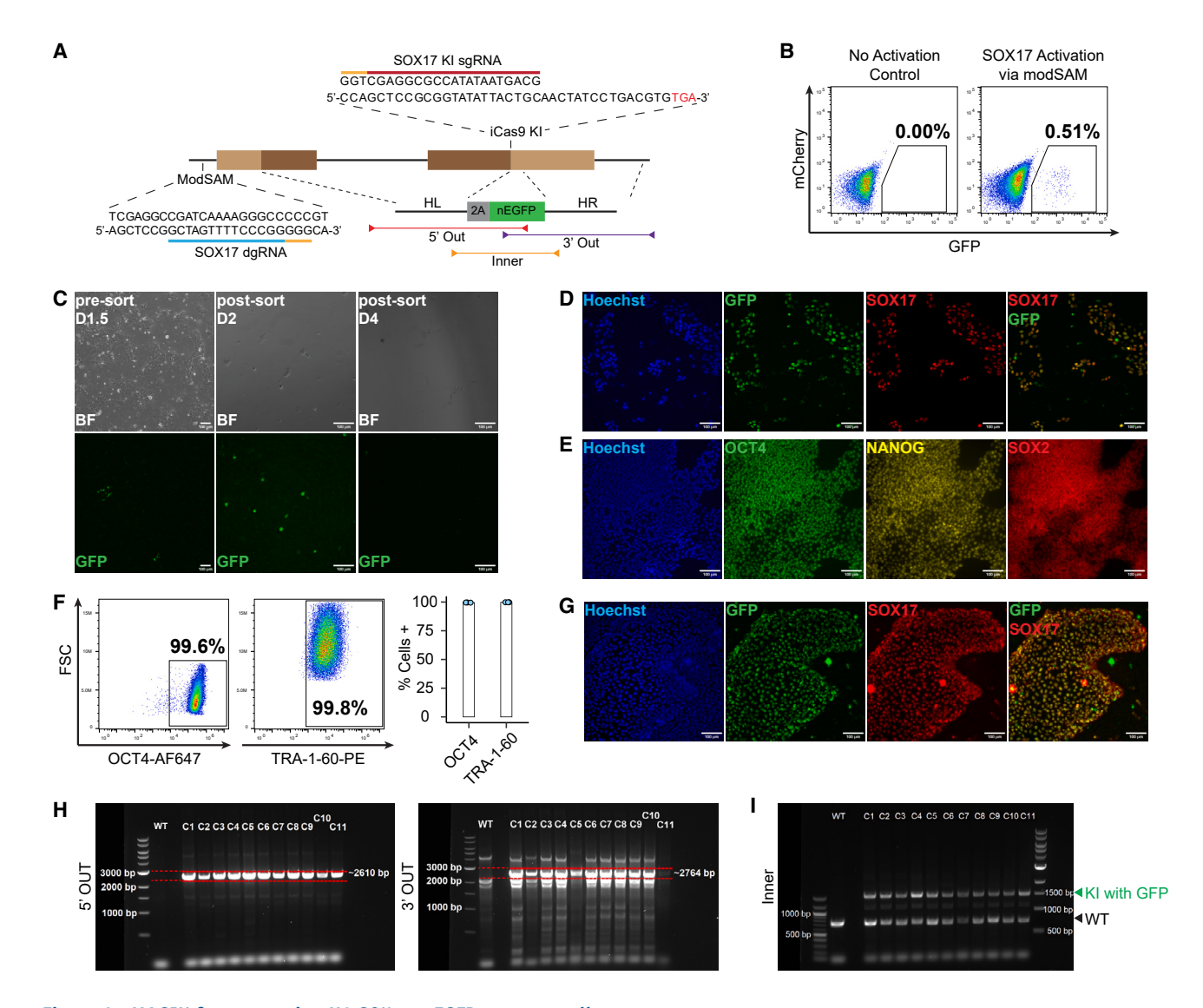


Figure 3. MAGIK for generating H9 SOX17-nEGFP reporter cells

- (A) Diagram showing knockin and activation strategy for SOX17.
- (B) WT H9 cells were transfected with iCas9 modRNA, SOX17 KI sqRNA, and SOX17-nEGFP mini-donor plasmid. The mixed knockin cells were transfected with dCas9 activator modRNA and SOX17 dqRNA. EGFP+ cells were sorted via FACS 48 h after transfection and replated into one well of a 48-well plate. Representative plot showing percentage of EGFP-positive cells.
- (C) Representative brightfield and fluorescent images of knockin reporter cells before and after sorting until day 4 post-transfection. Scale bar, 100 μM.
- (D) Post-sort H9 SOX17-nEGFP reporter cells were transfected with dCas9 activator modRNA and SOX17 dqRNA. On day 2 following transfection, cells were fixed and stained for SOX17. Representative fluorescent images showing co-localization of anti-SOX17 signal and EGFP. Scale bar, 100 μM.
- (E and F) Post-sort H9 SOX17-nEGFP reporter cells were stained for OCT4, NANOG, SOX2 and TRA-1-60 and analyzed by either immunofluorescent imaging (E) or flow cytometry (F). Scale bar, 100 µm. Representative flow cytometry plots and quantification of OCT4 and TRA-1-60 expression in post-sort H9 SOX17-nEGFP reporter cells. Error bars represent SEM across three independent experiments.
- (G) H9 SOX17-nEGFP reporter cells were differentiated to DE cells and then stained for SOX17. Representative fluorescent images showing co-localization of anti-SOX17 signal and EGFP. Scale bar, 100 µm.
- (H) PCR genotyping of 11 single-cell-derived clones from post-sort H9 SOX17-nEGFP reporter cells. The expected band from each set of primers is highlighted by a pair of red dashed lines (5' OUT, 2,610 bp; 3' OUT, 2,764 bp).
- (I) PCR genotyping of single-cell derived clones using Inner primers to distinguish between monoallelic and biallelic knockin (WT, 814 bp; KI with GFP, 1,615 bp).



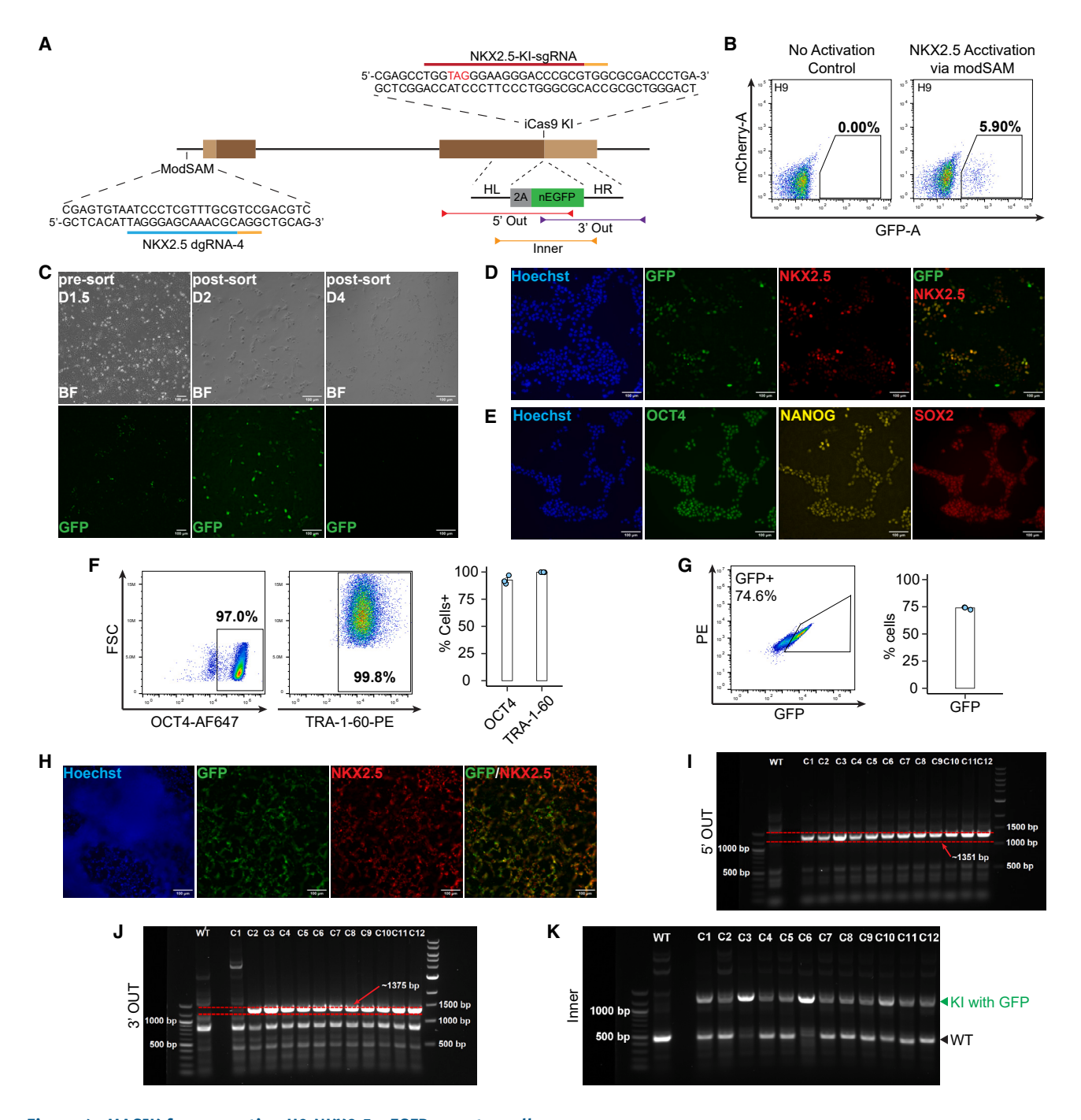


Figure 4. MAGIK for generating H9 NKX2.5-nEGFP reporter cells

- (A) Diagram showing knockin and activation strategy for NKX2.5.
- (B) WT H9 cells were transfected with iCas9 modRNA, NKX2.5 KI sgRNA, and NKX2.5-nEGFP mini-donor plasmid. Cells were expanded in TeSR for several days before being passaged into wells of a 12-well plate. The mixed knockin cells were transfected with dCas9 activator modRNA and NKX2.5 dgRNA. EGFP⁺ cells were sorted via FACS 48 h after transfection and replated into one well of a 48-well plate. Representative plot showing percentage of GFP-positive cells sorted from the total population.
- (C) Representative brightfield and fluorescent images of knockin reporter cells before and after sorting until day 4 after transfection. Scale bar, 100 μm.



PDX1 functions as a pivotal regulator in pancreas development (Kobayashi et al., 2010). During the differentiation of hPSCs into pancreatic lineages, the expression of PDX1 is observed in pancreatic progenitors and beta cells (Jiang et al., 2021; Randolph et al., 2019). In the context of PDX1 knockin, we leveraged our iCas9 modRNA in conjunction with a PDX1-EGFP mini-donor plasmid (Zhu et al., 2015) and a PDX1 KI sgRNA (Figure 5A). To effectively isolate cells that had undergone successful targeting, we transfected KI cells with our modSAM system, utilizing our validated dgRNA. Encouragingly, the MAGIK method yielded positive outcomes across all four cell lines. Two days after modSAM transfection, the proportions of EGFP+ cells were 0.44% (H9 hESC), 1.41% (IMR90 iPSC), 0.76% (H1 hESC), and 1.76% (6-9-9 iPSC) (Figures 5B, S3A, S4A, and S5A).

Subsequently, EGFP⁺-sorted cells were seeded into 1 well of a 48-well plate. Upon observation with a fluorescent microscope, it was confirmed that the attached cells were indeed expressing EGFP (Figures 5C, S3B, S3C, S4B, S4C, S5B, and S5C). As expected, all sorted cells ceased EGFP expression within one week of plating (Figures 5C, S3B, S3C, S4B, S4C, S5B, and S5C). Following expansion, the sorted cells underwent transfection with our modSAM system to activate PDX1 and EGFP expression. Immunostaining analyses showed co-localization between the EGFP signal and anti-PDX1 immunofluorescence signal (Figures 5D, S3D, S4D, and S5D). Moreover, the sorted cells consistently displayed nearly 100% expression of the pluripotency markers OCT4, NANOG, and SOX2, as determined through immunostaining across all tested cell lines (Figures 5E, S3E, S4E, and S5E). Additionally, the percentage of cells positive for OCT4 and TRA-1-60, as determined by flow cytometry, exhibited similarities between the sorted reporter cells and WT H9 cells (Figures 5F, S3F, S4F, and S5F). qPCR analysis of FACS-purified PDX1-EGFP H9 cells demonstrated robust expression of the canonical stem cell markers at levels similar to WT H9 cells (Figure S2A). These findings collectively signify the feasibility of using the MAGIK method to generate lineage-specific reporters within diverse hPSC populations.

Next, we differentiated PDX1-EGFP H9 cells into pancreatic β-cell using our small-molecule-based protocol (Jiang et al., 2021). At the end of stage 1, we obtained 58.8% FOXA2+ DE cells (Figure 5G). Additionally, at the end of stage 4, 31.6% of PDX1-EGFP reporter cells were EGFP⁺, indicating that our knockin reporter cells can accurately report the expression of PDX1 (Figure 5H). We further performed immunostaining of stage 4 cells using a PDX1 antibody. Our data showed co-localization of EGFP expression with the anti-PDX1 signal (Figure 5I). In addition to lineage-specific differentiation of the PDX1-EGFP reporter, we also performed neural induction of PDX1-EGFP reporter cells to demonstrate the fidelity of the reporter (Lippmann et al., 2014). As expected, after neural differentiation, H9 PDX1-EGFP cells showed robust expression of the neuroectoderm fate marker PAX6 and no EGFP expression on day 10 of differentiation similar to WT H9 cells—as determined by immunostaining and qPCR analysis (Figures S2B and S2C).

We derived multiple single-cell clonal populations from our sorted H9, H1, and IMR90 PDX1-EGFP reporters and extracted gDNA for PCR analysis. Using our 5' Out and 3' Out probes, we showed successful amplification of the expected bands, demonstrating successful integration of the fluorescent reporter at the target site across all clonal populations in all three cell lines (Figures 5J, 5K. S3G, and S4G). Additionally, PCR amplification of the gDNA using the Inner primers indicated that 5 clonal lines out of the 32 clonal populations tested across the three cell lines (15.6%) were homozygous for reporter integration (Figures 5L, S3H, and S4H).

Overall, we showed that our MAGIK method can be used to derive fluorescent reporter lines across multiple lineagespecific genes and demonstrated the robustness of MAGIK across multiple hPSC lines.

⁽D) Post-sort H9 NKX2.5-nEGFP reporter cells were transfected with dCas9 activator modRNA and NKX2.5 dqRNA. On day 2 following transfection, cells were fixed and stained for NKX2.5 (red). Representative fluorescent images showing co-localization of anti-NKX2.5 signal and GFP. Scale bar, 100 μm.

⁽E and F) Post-sort H9-NKX2.5nEGFP reporter cells were stained for OCT4, NANOG, SOX2 and TRA-1-60 and analyzed by either immunofluorescent imaging (E) or flow cytometry (F). Scale bar, 100 µm. Representative flow cytometry plots and quantification of OCT4 and TRA-1-60 expression in post-sort H9 NKX2.5-nEGFP reporter cells. Error bars represent SEM across three independent experiments.

⁽G and H) H9 NKX2.5-nEGFP reporter cells were seeded on Matrigel-coated plates and differentiated into cardiomyocytes using our GiWi protocol. Day 10 cells were either (G) collected for live-cell flow cytometry or (H) fixed and stained for NKX2.5 for immunofluorescent imaging. (G) Representative flow cytometry plot and quantification of EGFP expression. Error bars represent SEM across three replicates.

⁽I and J) PCR genotyping of 12 single-cell derived clones from post-sort H9 NKX2.5-nEGFP reporter cells. The expected band from each set of probes is highlighted by a pair of red dashed lines (5' OUT, 1,351 bp; 3' OUT, 1,375 bp).

⁽K) PCR genotyping of single-cell derived clones using Inner primers to distinguish between mono-allelic and bi-allelic integration of the fluorescent reporter (WT, 499 bp; KI with GFP, 1,303 bp).



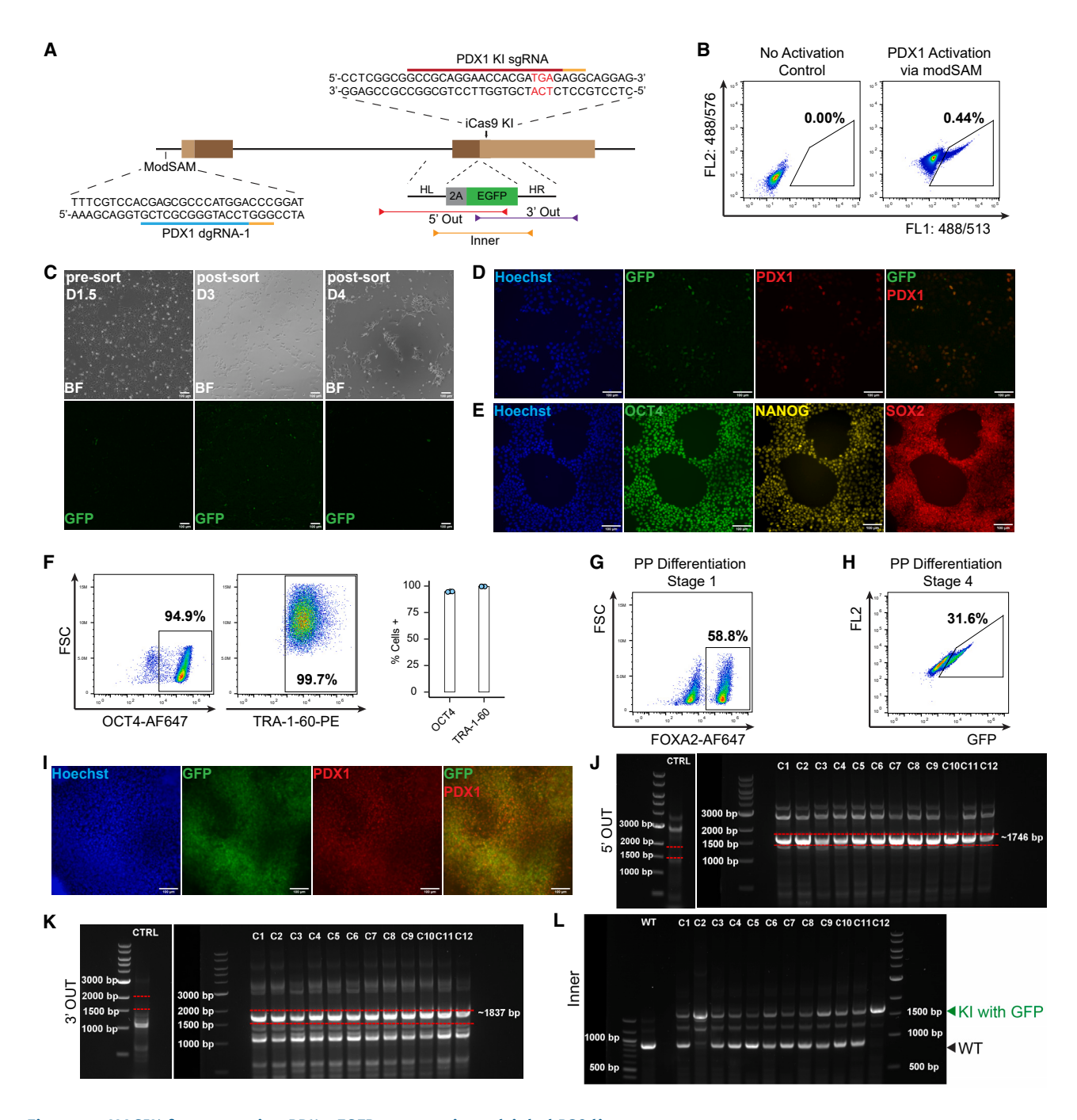


Figure 5. MAGIK for generating PDX1-EGFP reporter in multiple hPSC lines

- (A) Diagram showing knockin and activation strategy for PDX1.
- (B) WT H9 cells were transfected with iCas9 modRNA, PDX1 KI sgRNA, and PDX1-EGFP mini-donor plasmid. Cells were expanded in TeSR for several days before being passaged into multiple wells of a 12-well plate. The mixed knockin cells were transfected with dCas9 activator modRNA and PDX1 dgRNA. EGFP⁺ cells were sorted via FACS 48 h after transfection and replated into one well of a 48-well plate. Representative plot showing percentage of EGFP-positive cells sorted from the total population.
- (C) Representative brightfield and fluorescent images of knockin reporter cells before and after sorting until day 4 after transfection. Scale bar, 100 μm.
- (E) Post-sort H9 PDX1-EGFP reporter cells were transfected with dCas9 activator modRNA and PDX1 dgRNA. On day 2 following transfection, cells were fixed and stained for PDX1. Representative fluorescent images showing co-localization of anti-PDX1 signal and EGFP. Scale bar, 100 μm. (E and F) Post-sort H9 PDX1-EGFP reporter cells were stained for OCT4, NANOG, SOX2, and TRA-1-60 and analyzed by either (legend continued on next page)



DISCUSSION

The ability to perform knockin in hPSCs is vital for the advancement of stem cell research and therapy. The introduction of fluorescent proteins into lineage-specific marker genes within hPSCs has revolutionized the isolation of desired differentiated cells. However, conventional knockin methodologies have long grappled with challenges like low efficiency and intricate protocols. The necessity of integrating a drug-selection cassette into the donor plasmid, coupled with the subsequent requirement to excise the drug selection component post-successful knockin, has elongated the knockin process significantly.

Scientists have developed various strategies to enhance the efficiency of precise sequence replacement or insertion via HDR. By strategically designing ssDNA donors with optimal length complementary to the strand initially released by Cas9, researchers can boost HDR rates in human cells, achieving rates as high as 60% (Richardson et al., 2016). However, synthesizing long ssDNA poses relative difficulty. For using dsDNA donors, researchers have discovered that modifying dsDNA, such as using specially designed 3' overhang dsDNA donors containing 50-nt homology arms (Han et al., 2023) or using sgRNA-PAM sequence-flanked dsDNA as donors (Zhang et al., 2017), can significantly enhance HDR efficiency. These specialized dsDNA donors have not been demonstrated in hPSCs and these special donors present greater production challenges compared with traditional plasmid donors. Additionally, researchers have explored small-molecule inhibitors to enhance HDR efficiency. They identified AZD7648, an inhibitor of DNA-dependent protein kinase catalytic subunit, a crucial protein in the alternative repair pathway of nonhomologous end-joining, which can substantially increase HDR efficiency (up to 50-fold) (Selvaraj et al., 2023). Simultaneously inhibiting DNA-PK and Pol⊕ can further improve HDR efficiency and the precision of genome editing (Wimberger et al., 2023). Nevertheless, despite these multiple approaches to enhance HDR efficiency, it is important to note that HDR efficiency is not guaranteed to reach 100%.

Consequently, achieving precise integration of a fluorescent protein into a silenced lineage-specific marker gene still necessitates single cell cloning, a step that considerably delays the knockin process.

To address these challenges, we introduce the MAGIK method. This novel strategy enhances knockin efficiency by using an iCas9 modRNA and facilitates target cell isolation with a modSAM system. Our method simplifies the process of isolating successful knockin cells, providing a markedly efficient and expedited alternative to conventional methods. The MAGIK method stands out for its efficiency and simplicity. It starts with the use of an iCas9 modRNA to significantly enhance knockin efficiency. The subsequent step uses a dCas9 activator modRNA to temporarily activate the expression of lineage-specific genes and their associated fluorescent proteins, simplifying the isolation of correctly targeted cells through FACS. According to our data, all FACS-sorted EGFP+ cells (100%) are correctly targeted clones, with some being biallelic targeting clones.

The MAGIK results showed a 45-fold improvement over an entirely plasmid-based approach. We demonstrate the robustness of MAGIK across multiple lineage-specific genes (NKX6.1, SOX17, NKX2.5, and PDX1) and four hPSC lines. The method's ability to derive relatively pure fluorescent reporter cells without the use of drug selection cassettes and arduous genomic PCR screening makes it a significant advancement in the field.

In summary, the MAGIK method represents a significant step forward in the field of stem cell research. Its efficiency, simplicity, and applicability across various genes and stem cell lines make it a promising tool for developing lineagespecific reporters. The future applications of MAGIK could extend to various areas of biomedical research, offering new avenues for understanding and treating human diseases.

Limitations of the study

While we are able to achieve relatively pure populations of correctly targeted lineage-specific fluorescent reporter hPSCs via our MAGIK method, some researchers may opt to derive single-cell clones for the purpose of establishing

immunofluorescent imaging (E) or flow cytometry (F). Scale bar, 100 µm. Representative flow cytometry plots and quantification of OCT4 and TRA-1-60 expression in post-sort H9 PDX1-EGFP reporter cells. Error bars represent SEM across three independent experiments. (G and I) H9 PDX1-EGFP reporter cells were differentiated to pancreatic progenitors (PPs) using our GiBi protocol. (G) Day 4 cells were collected and analyzed for FOXA2 expression by flow cytometry.

⁽H) Day 14 cells were collected and analyzed for EGFP expression by flow cytometry.

⁽I) Day 14 cells were fixed and stained for PDX1. Representative fluorescent images showing colocalization of anti-PDX1 signal and EGFP.

⁽J and K) PCR genotyping of 12 single-cell-derived clones from post-sort H9 PDX1-EGFP reporter cells. Expected band from each set of probes is highlighted by a pair of red dashed lines (5' OUT, 1,746 bp; 3' OUT, 1,837 bp).

⁽L) PCR genotyping of single cell derived clones using Inner primers to distinguish between monoallelic and biallelic knock in (WT, 885 bp; KI with GFP, 1,659 bp).



bi-allelic knockins. While the transient activation of the lineage-specific genes targeted in this study did not induce differentiation, it is conceivable that activating certain genes transiently might lead to pluripotency loss. This potential outcome could pose challenges in isolating accurately targeted cells using the MAGIK method.

An additional constraint of our method is the necessity for robust activation of the target gene to facilitate FACS isolation. Although CRISPRa systems have been extensively used for activating numerous genes, optimal dgRNAs for some genes remain undetermined. To target novel genes, researchers may need to screen multiple dgRNAs to identify the optimal combination. Fortunately, ongoing advancements in CRISPRa systems and online tools like CHOPCHOP for dgRNA selection are simplifying this process (Armando Casas-Mollano et al., 2020; Labun et al., 2019).

EXPERIMENTAL PROCEDURES

Resource availability

Lead contact

Further information and requests for resources and reagents should be directed to and will be fulfilled by the lead contact, Dr. Lian (Lian@psu.edu).

Materials availability

We have deposited our newly generated plasmids to Addgene with the catalog number: modRNAc1-Cas9-2A-Puro (216390), mod-RNAc1-Cas9-2A-p53DD (216389), modRNAc1-VP64dCas9VP64-2A-MPH (216388), mini-donor NKX6.1-2A-nEGFP (206047), mini-donor SOX17-2A-nEGFP (206048), and mini-donor NKX2.5-2A-nEGFP (209287).

Data and code availability

- The published article includes all the dataset generated during this study.
- $\bullet\,$ This paper does not report original code.
- Any additional information required to re-analyze the data reported in this paper is available from the lead contact upon request.

ModRNA or plasmid-based knockin in hPSCs

For knockin, approximately 14,000 cells/cm² hPSCs were seeded onto iMatrix-511 coated wells of a 12-well plate and cultured for 24 h at 37°C, 5% CO₂. For modRNA-based knockin, iCas9 modRNA, KI sgRNA, and mini-donor plasmid were combined with Lipofectamine Stem Transfection Reagent (Thermo Fisher Scientific) (1:4 ratio, mass/volume) in Opti-MEM media. For plasmid-based knockin, iCas9 modRNA was replaced with the EFS-Cas9 plasmid. Before transfection, the spent culture medium was replaced with fresh TeSR supplemented with 10 μ M Y-27632. The transfection mix was incubated at room temperature for 10 min before being added to the well in a dropwise fashion. The transfection media was changed 24 h later, and cells were maintained in TeSR with daily media changes.

ModSAM-mediated target gene activation in hPSCs

For modSAM-mediated gene activation, approximately 28,000 cells/ cm² hPSCs were seeded onto iMatrix-511-coated wells of a 12-well plate and cultured for 24 h at 37°C, 5% CO2. For modRNA-based activation, the dCas9 activator modRNA and dgRNA were combined with Lipofectamine Stem Transfection Reagent (1:4 ratio, mass/ volume) in Opti-MEM medium. For plasmid-based activation, the dCas9 activator modRNA was replaced with pPB-R1R2-EF1a-VP64dCas9VP64-T2A-MS2p65HSF1-IRES-bsd-pA plasmid (Addgene, #113341). Before transfection, the spent culture medium was replaced with fresh TeSR supplemented with 10 μ M Y-27632. The transfection mix was incubated at room temperature for 10 min before being added to the well in a dropwise fashion followed by a media change 24 h later. Cells were collected between 36 and 48 h after transfection for either FACS or flow cytometry.

Statistical analysis

Quantification of flow cytometry data is shown as the mean \pm SEM unless otherwise specified. All statistical analyses were performed in R. Unpaired Student's t-test was used for comparison between two groups. For comparison between multiple groups a two-way ANOVA followed by *post hoc* Tukey's test was used. A value of p>0.05 was considered not significant; *p<0.05, **p<0.01, and ****p<0.001 were considered statistically significant.

SUPPLEMENTAL INFORMATION

Supplemental information can be found online at https://doi.org/10.1016/j.stemcr.2024.03.005.

ACKNOWLEDGMENTS

This work was supported by NSF CBET-1943696 (to X.L.L.), NSF CBET-2319913 (to X.L.L.), NSF CBET-2143064 (to X.B.), NIH R21EB026035 (to X.L.L.), NIH R56DK133147 (to X.L.L.), Huck Innovative and Transformational Seed (HITS) Fund (to X.L.L.), and NIH R37CA265926 (to X.B.).

AUTHOR CONTRIBUTIONS

T.H. and X.L.L. designed the experiments and analyzed the results. T.H. and J.L. performed the experiments and analyzed data. X.L.L. supervised the experiments. T.H. and X.L.L. wrote the manuscript. T.H., X.B., and X.L.L. contributed to the revision of the manuscript.

DECLARATION OF INTERESTS

All authors declare no competing interests.

Received: March 1, 2024 Revised: March 8, 2024 Accepted: March 8, 2024 Published: April 4, 2024



REFERENCES

Armando Casas-Mollano, J., Zinselmeier, M.H., Erickson, S.E., and Smanski, M.J. (2020). CRISPR-Cas Activators for Engineering Gene Expression in Higher Eukaryotes. Cris. J. 3, 350–364.

Azhagiri, M.K.K., Babu, P., Venkatesan, V., and Thangavel, S. (2021). Homology-directed gene-editing approaches for hematopoietic stem and progenitor cell gene therapy. Stem Cell Res.

Bak, R.O., and Porteus, M.H. (2017). CRISPR-Mediated Integration of Large Gene Cassettes Using AAV Donor Vectors. Cell Rep. 20, 750-756.

Banan, M. (2020). Recent advances in CRISPR/Cas9-mediated knock-ins in mammalian cells. J. Biotechnol. 308, 1-9.

Bao, X., Adil, M.M., Muckom, R., Zimmermann, J.A., Tran, A., Suhy, N., Xu, Y., Sampayo, R.G., Clark, D.S., and Schaffer, D.V. (2019). Gene Editing to Generate Versatile Human Pluripotent Stem Cell Reporter Lines for Analysis of Differentiation and Lineage Tracing. Stem Cell. 37, 1556-1566.

Cabrera, A., Edelstein, H.I., Glykofrydis, F., Love, K.S., Palacios, S., Tycko, J., Zhang, M., Lensch, S., Shields, C.E., Livingston, M., et al. (2022). The sound of silence: Transgene silencing in mammalian cell engineering. Cell Syst. 13, 950-973.

Capecchi, M.R. (1989). Altering the Genome by Homologous Recombination. Science 244, 1288-1292.

Chavez, A., Tuttle, M., Pruitt, B.W., Ewen-Campen, B., Chari, R., Ter-Ovanesyan, D., Haque, S.J., Cecchi, R.J., Kowal, E.J.K., Buchthal, J., et al. (2016). Comparison of Cas9 activators in multiple species. Nat. Methods 13, 563-567.

Cong, L., Ran, F.A., Cox, D., Lin, S., Barretto, R., Habib, N., Hsu, P.D., Wu, X., Jiang, W., Marraffini, L.A., and Zhang, F. (2013). Multiplex genome engineering using CRISPR/Cas systems. Science 339, 819-823.

Cruz-Santos, M., Cardo, L.F., and Li, M. (2022). A Novel LHX6 Reporter Cell Line for Tracking Human iPSC-Derived Cortical Interneurons. Cells 11.

D'Amour, K.A., Agulnick, A.D., Eliazer, S., Kelly, O.G., Kroon, E., and Baetge, E.E. (2005). Efficient differentiation of human embryonic stem cells to definitive endoderm. Nat. Biotechnol. 23, 1534-1541.

Elliott, D.A., Braam, S.R., Koutsis, K., Ng, E.S., Jenny, R., Lagerqvist, E.L., Biben, C., Hatzistavrou, T., Hirst, C.E., Yu, Q.C., et al. (2011). NKX2-5 eGFP/w hESCs for isolation of human cardiac progenitors and cardiomyocytes. Nat. Methods 8, 1037-1040.

Gaj, T., Staahl, B.T., Rodrigues, G.M.C., Limsirichai, P., Ekman, F.K., Doudna, J.A., and Schaffer, D.V. (2017). Targeted gene knock-in by homology-directed genome editing using Cas9 ribonucleoprotein and AAV donor delivery. Nucleic Acids Res. 45, e98.

Haideri, T., Howells, A., Jiang, Y., Yang, J., Bao, X., and Lian, X.L. (2022). Robust genome editing via modRNA-based Cas9 or base editor in human pluripotent stem cells. Cell Rep. Methods 2, 100290.

Han, W., Li, Z., Guo, Y., He, K., Li, W., Xu, C., Ge, L., He, M., Yin, X., Zhou, J., et al. (2023). Efficient precise integration of large DNA sequences with 3'-overhang dsDNA donors using CRISPR/Cas9. Proc. Natl. Acad. Sci. USA 120, e2221127120.

Den Hartogh, S.C., and Passier, R. (2016). Fluorescent Reporters in Human Pluripotent Stem Cells: Contributions to Cardiac Differentiation and Their Applications in Cardiac Disease and Toxicity. Stem Cell. 34, 13-26.

Herbst, F., Ball, C.R., Tuorto, F., Nowrouzi, A., Wang, W., Zavidij, O., Dieter, S.M., Fessler, S., Van Der Hoeven, F., Kloz, U., et al. (2012). Extensive methylation of promoter sequences silences lentiviral transgene expression during stem cell differentiation in vivo. Mol. Ther. 20, 1014-1021.

Hsu, P.D., Lander, E.S., and Zhang, F. (2014). Development and applications of CRISPR-Cas9 for genome engineering. Cell 157, 1262-1278.

Irie, N., Weinberger, L., Tang, W.W.C., Kobayashi, T., Viukov, S., Manor, Y.S., Dietmann, S., Hanna, J.H., and Surani, M.A. (2015). SOX17 is a critical specifier of human primordial germ cell fate. Cell 160, 253-268.

Jiang, Y., Chen, C., Randolph, L.N., Ye, S., Zhang, X., Bao, X., and Lian, X.L. (2021). Generation of pancreatic progenitors from human pluripotent stem cells by small molecules. Stem Cell Rep. 16, 2395-2409.

Jinek, M., Chylinski, K., Fonfara, I., Hauer, M., Doudna, J.A., and Charpentier, E. (2012). A Programmable Dual-RNA – Guided DNA Endonuclease in Adaptive Bacterial Immunity. Science (80-337, 816-821.

Jung, H.S., Uenishi, G., Park, M.A., Liu, P., Suknuntha, K., Raymond, M., Choi, Y.J., Thomson, J.A., Ong, I.M., and Slukvin, I.I. (2021). SOX17 integrates HOXA and arterial programs in hemogenic endothelium to drive definitive lympho-myeloid hematopoiesis. Cell Rep. 34, 108758.

Kagita, A., Lung, M.S.Y., Xu, H., Kita, Y., Sasakawa, N., Iguchi, T., Ono, M., Wang, X.H., Gee, P., and Hotta, A. (2021). Efficient ssODN-Mediated Targeting by Avoiding Cellular Inhibitory RNAs through Precomplexed CRISPR-Cas9/sgRNA Ribonucleoprotein. Stem Cell Rep. 16, 985-996.

Kiani, S., Chavez, A., Tuttle, M., Hall, R.N., Chari, R., Ter-Ovanesyan, D., Qian, J., Pruitt, B.W., Beal, J., Vora, S., et al. (2015). Cas9 gRNA engineering for genome editing, activation and repression. Nat. Methods 12, 1051-1054.

Kobayashi, T., Yamaguchi, T., Hamanaka, S., Kato-Itoh, M., Yamazaki, Y., Ibata, M., Sato, H., Lee, Y.S., Usui, J.I., Knisely, A.S., et al. (2010). Generation of rat pancreas in mouse by interspecific blastocyst injection of pluripotent stem cells. Cell 142, 787–799.

Konermann, S., Brigham, M.D., Trevino, A.E., Joung, J., Abudayyeh, O.O., Barcena, C., Hsu, P.D., Habib, N., Gootenberg, J.S., Nishimasu, H., et al. (2015). Genome-scale transcriptional activation by an engineered CRISPR-Cas9 complex. Nature 517, 583-588.

Labun, K., Montague, T.G., Krause, M., Torres Cleuren, Y.N., Tjeldnes, H., and Valen, E. (2019). CHOPCHOP v3: Expanding the CRISPR web toolbox beyond genome editing. Nucleic Acids Res. 47, W171-W174.

Lau, C.-H., Tin, C., and Suh, Y. (2020). CRISPR-based strategies for targeted transgene knock-in and gene correction. Fac. Rev. 9, 20.



Lee, K., Cho, H., Rickert, R.W., Li, Q.V., Pulecio, J., Leslie, C.S., and Huangfu, D. (2019). FOXA2 Is Required for Enhancer Priming during Pancreatic Differentiation. Cell Rep. *28*, 382–393.e7.

Lian, X., Hsiao, C., Wilson, G., Zhu, K., Hazeltine, L.B., Azarin, S.M., Raval, K.K., Zhang, J., Kamp, T.J., and Palecek, S.P. (2012). Robust cardiomyocyte differentiation from human pluripotent stem cells via temporal modulation of canonical Wnt signaling. Proc. Natl. Acad. Sci. *109*, E1848–E1857.

Lian, X., Zhang, J., Azarin, S.M., Zhu, K., Hazeltine, L.B., Bao, X., Hsiao, C., Kamp, T.J., and Palecek, S.P. (2013). Directed cardiomyocyte differentiation from human pluripotent stem cells by modulating Wnt/ β -catenin signaling under fully defined conditions. Nat. Protoc. *8*, 162–175.

Liao, H.-K., Hatanaka, F., Araoka, T., Reddy, P., Wu, M.-Z., Sui, Y., Yamauchi, T., Sakurai, M., O'Keefe, D.D., Núñez-Delicado, E., et al. (2017). Vivo Target Gene Activation via CRISPR/Cas9-Mediated Trans-epigenetic Modulation. Cell *171*, 1495–1507.e15.

Lippmann, E.S., Estevez-Silva, M.C., and Ashton, R.S. (2014). Defined human pluripotent stem cell culture enables highly efficient neuroepithelium derivation without small molecule inhibitors. Stem Cell. *32*, 1032–1042.

Liu, H., Li, R., Liao, H.K., Min, Z., Wang, C., Yu, Y., Shi, L., Dan, J., Hayek, A., Martinez Martinez, L., et al. (2021). Chemical combinations potentiate human pluripotent stem cell-derived 3D pancreatic progenitor clusters toward functional β cells. Nat. Commun. *12*.

Liu, Y., Hermes, J., Li, J., and Tudor, M. (2018). Endogenous locus reporter assays. In Methods in Molecular Biology (Humana Press Inc.), pp. 163–177.

Mali, P., Yang, L., Esvelt, K.M., Aach, J., Guell, M., DiCarlo, J.E., Norville, J.E., and Church, G.M. (2013). RNA-guided human genome engineering via Cas9. Science *339*, 823–826.

Martyn, I., Kanno, T.Y., Ruzo, A., Siggia, E.D., and Brivanlou, A.H. (2018). Self-organization of a human organizer by combined Wnt and Nodal signalling. Nature *558*, 132–135.

Merkle, F.T., Neuhausser, W.M., Santos, D., Valen, E., Gagnon, J.A., Maas, K., Sandoe, J., Schier, A.F., and Eggan, K. (2015). Efficient CRISPR-Cas9-Mediated Generation of Knockin Human Pluripotent Stem Cells Lacking Undesired Mutations at the Targeted Locus. Cell Rep. *11*, 875–883.

Mikkelsen, N.S., Hernandez, S.S., Jensen, T.I., Schneller, J.L., and Bak, R.O. (2023). Enrichment of transgene integrations by transient CRISPR activation of a silent reporter gene. Mol. Ther. Methods Clin. Dev. *29*, 1–16.

Okamoto, S., Amaishi, Y., Maki, I., Enoki, T., and Mineno, J. (2019). Highly efficient genome editing for single-base substitutions using optimized ssODNs with Cas9-RNPs. Sci. Rep. *9*, 4811.

Ovchinnikov, D.A., Titmarsh, D.M., Fortuna, P.R.J., Hidalgo, A., Alharbi, S., Whitworth, D.J., Cooper-White, J.J., and Wolvetang, E.J. (2014). Transgenic human ES and iPS reporter cell lines for identification and selection of pluripotent stem cells in vitro. Stem Cell Res. *13*, 251–261.

Pagliuca, F., Millman, J., Gürtler, M., Segel, M., Van Dervort, A., Ryu, J., Peterson, Q., Van Dervort, A., Melton, D., Van Dervort,

A., et al. (2014). Generation of functional human pancreatic β cells in vitro. Cell *159*, 428–439.

Randolph, L.N., Bhattacharyya, A., and Lian, X.L. (2019). Human beta cells generated from pluripotent stem cells or cellular reprogramming for curing diabetes. Regen. Eng. Transl. Med. *5*, 42–52.

Reamon-Buettner, S.M., and Borlak, J. (2010). NKX2-5: An update on this hypermutable homeodomain protein and its role in human congenital heart disease (CHD). Hum. Mutat. *31*, 1185–1194.

Richardson, C.D., Ray, G.J., DeWitt, M.A., Curie, G.L., and Corn, J.E. (2016). Enhancing homology-directed genome editing by catalytically active and inactive CRISPR-Cas9 using asymmetric donor DNA. Nat. Biotechnol. *34*, 339–344.

Selvaraj, S., Feist, W.N., Viel, S., Vaidyanathan, S., Dudek, A.M., Gastou, M., Rockwood, S.J., Ekman, F.K., Oseghale, A.R., Xu, L., et al. (2023). High-efficiency transgene integration by homology-directed repair in human primary cells using DNA-PKcs inhibition. Nat. Biotechnol. https://doi.org/10.1038/s41587-023-01888-4.

Sluch, V.M., Davis, C.H.O., Ranganathan, V., Kerr, J.M., Krick, K., Martin, R., Berlinicke, C.A., Marsh-Armstrong, N., Diamond, J.S., Mao, H.Q., and Zack, D.J. (2015). Differentiation of human ESCs to retinal ganglion cells using a CRISPR engineered reporter cell line. Sci. Rep. *5*, 16595.

Sun, W.S., Chun, J.L., Do, J.T., Kim, D.H., Ahn, J.S., Kim, M.K., Hwang, I.S., Kwon, D.J., Hwang, S.S., and Lee, J.W. (2016). Construction of a Dual-Fluorescence Reporter System to Monitor the Dynamic Progression of Pluripotent Cell Differentiation. Stem Cells Int *2016*, 1390284.

Wimberger, S., Akrap, N., Firth, M., Brengdahl, J., Engberg, S., Schwinn, M.K., Slater, M.R., Lundin, A., Hsieh, P.-P., Li, S., et al. (2023). Simultaneous inhibition of DNA-PK and Pol Θ improves integration efficiency and precision of genome editing. Nat. Commun. *14*, 4761.

Wu, W., Liu, J., Su, Z., Li, Z., Ma, N., Huang, K., Zhou, T., and Wang, L. (2018). Generation of H1 PAX6WT/EGFP reporter cells to purify PAX6 positive neural stem/progenitor cells. Biochem. Biophys. Res. Commun. *502*, 442–449.

Xia, X., Zhang, Y., Zieth, C.R., and Zhang, S.C. (2007). Transgenes delivered by lentiviral vector are suppressed in human embryonic stem cells in a promoter-dependent manner. Stem Cells Dev. *16*, 167–176.

Yoshimi, K., Kunihiro, Y., Kaneko, T., Nagahora, H., Voigt, B., and Mashimo, T. (2016). SSODN-mediated knock-in with CRISPR-Cas for large genomic regions in zygotes. Nat. Commun. *7*, 10431.

Yu, Y., Guo, Y., Tian, Q., Lan, Y., Yeh, H., Zhang, M., Tasan, I., Jain, S., and Zhao, H. (2020). An efficient gene knock-in strategy using 5'-modified double-stranded DNA donors with short homology arms. Nat. Chem. Biol. *16*, 387–390.

Zhang, J.P., Li, X.L., Li, G.H., Chen, W., Arakaki, C., Botimer, G.D., Baylink, D., Zhang, L., Wen, W., Fu, Y.W., et al. (2017). Efficient precise knockin with a double cut HDR donor after CRISPR/Cas9-mediated double-stranded DNA cleavage. Genome Biol. *18*, 35.

Zhu, Z., Verma, N., González, F., Shi, Z.D., and Huangfu, D. (2015). A CRISPR/Cas-Mediated Selection-free Knockin Strategy in Human Embryonic Stem Cells. Stem Cell Rep. *4*, 1103–1111.